

---

# Fence off Anomaly Interference: Cross-Domain Distillation for Fully Unsupervised Anomaly Detection

---

Anonymous Author(s)

Affiliation

Address

email

1 In the supplementary material, we organize the content into the following sections:

- 2 • Appendix A provides intuitive visualization evidence for the motivation of our method.
- 3 • Appendix B presents results on VisA with different noise ratios.
- 4 • Appendix C details the algorithm.
- 5 • Appendix D includes additional parameter ablation study results.
- 6 • Appendix E reports quantitative results for each category on MVTec AD and VisA.
- 7 • Appendix F offers more visualization results of the generated anomaly maps.
- 8 • Appendix G discusses limitations and proposes future work.

## 9 A Visualizations for Motivation

### 10 A.1 Discussion of the Effectiveness of RD for FUAD

11 In Sec. 3.1, we discuss why Reverse Distillation (RD) is able to be applied to the Fully Unsupervised  
12 Anomaly Detection (FUAD) task, including the Probability Perspective (normal samples dominate)  
13 and the Distribution Perspective (normal sample distribution is concentrated, while anomalous  
14 distribution is dispersed).

15 Fig. A1 presents t-SNE visualizations of teacher features for three MVTec [1] categories: carpet,  
16 grid, and leather. Green points represent features of normal pixels, and red points represent features  
17 of anomalous pixels. The visualizations confirm that features of normal pixels are the majority and  
18 clustered, while features of anomalous pixels are typically distant from the normal distribution center,  
19 appearing as outliers.

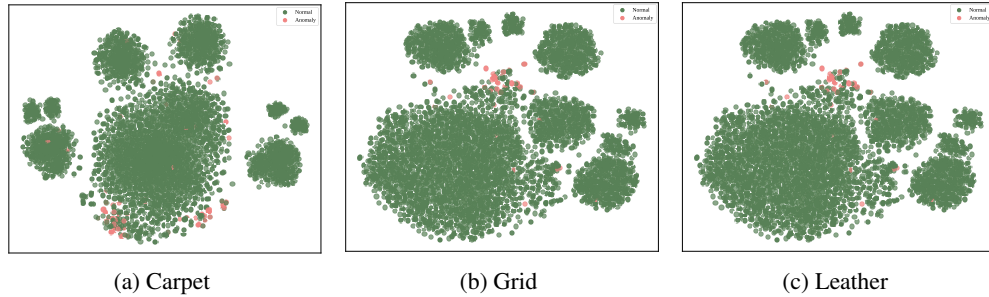


Figure A1: The t-SNE diagrams of feature distribution corresponding to the categories carpet, grid and leather in MVTec AD.

## 20 A.2 Intuitive Evidence of Cross-Domain Distillation

21 To intuitively demonstrate the feasibility of our proposed Cross-Domain Distillation for the FUAD  
 22 task, we conduct toy experiments on three categories from the MVTec dataset: cable, metal nut, and  
 23 transistor, as shown in Fig. A2, Fig. A3, and Fig. A4.

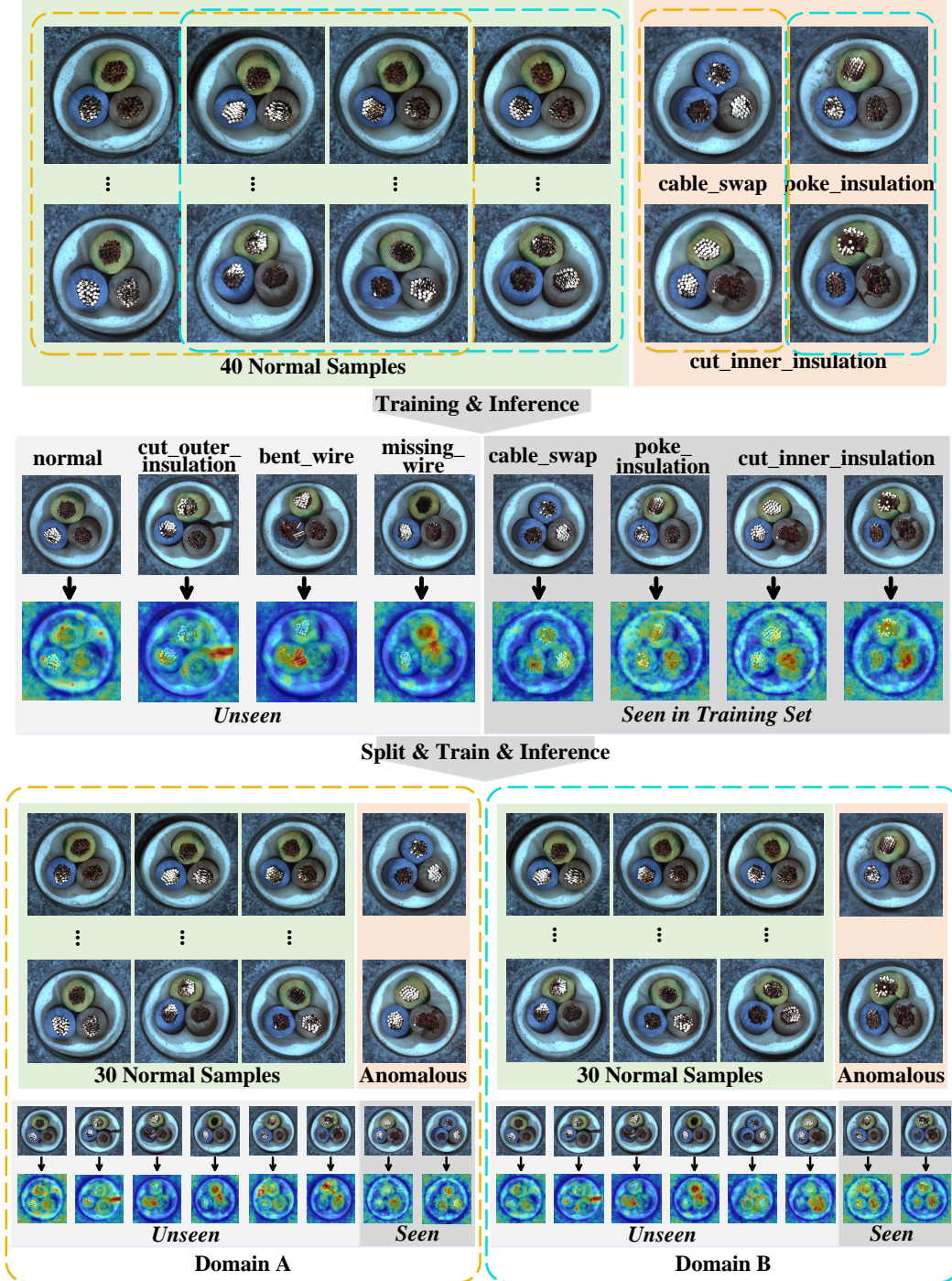


Figure A2: Results of the toy experiment for the category *cable*.



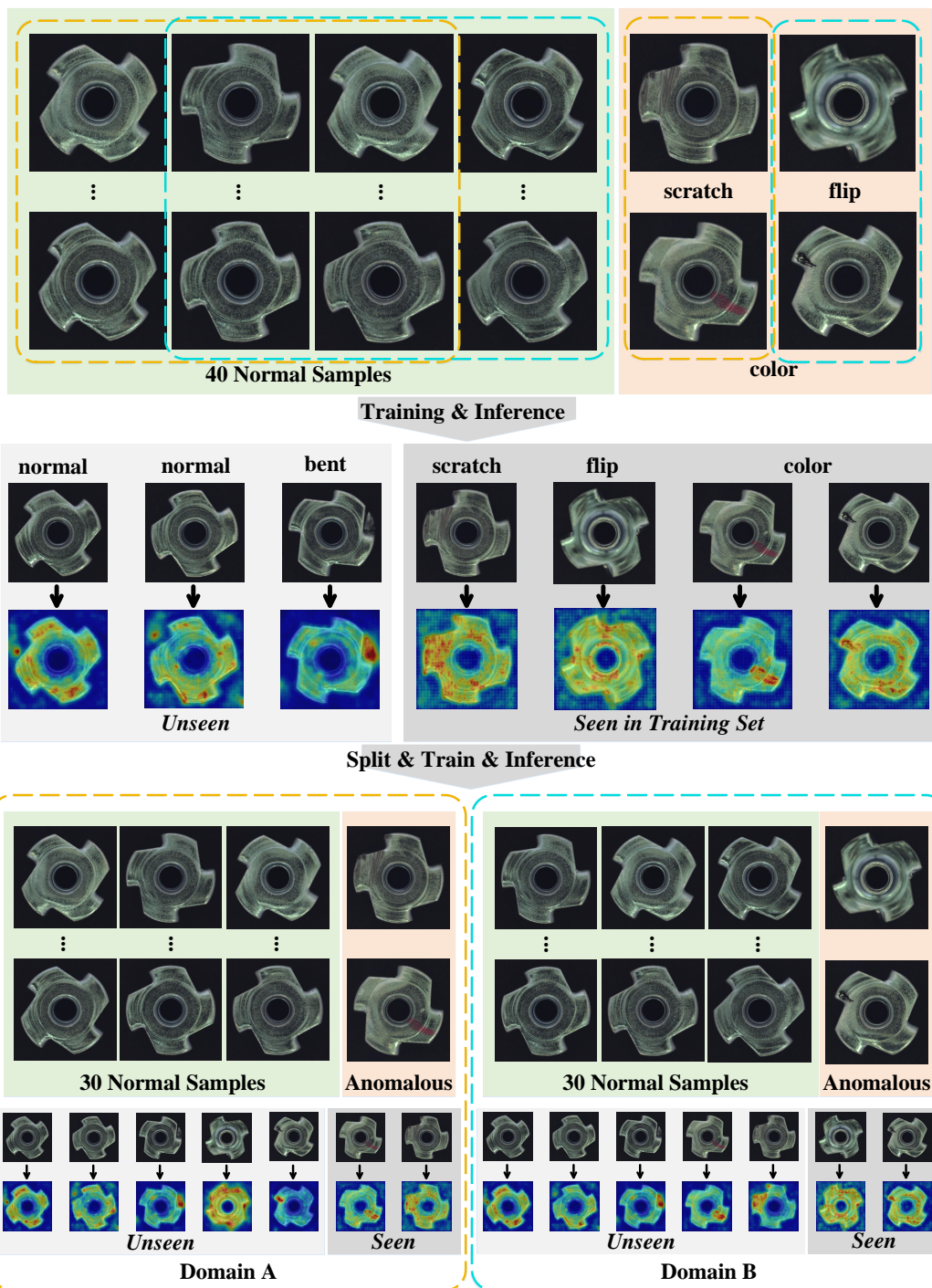


Figure A3: Results of the toy experiment for the category *metal nut*.

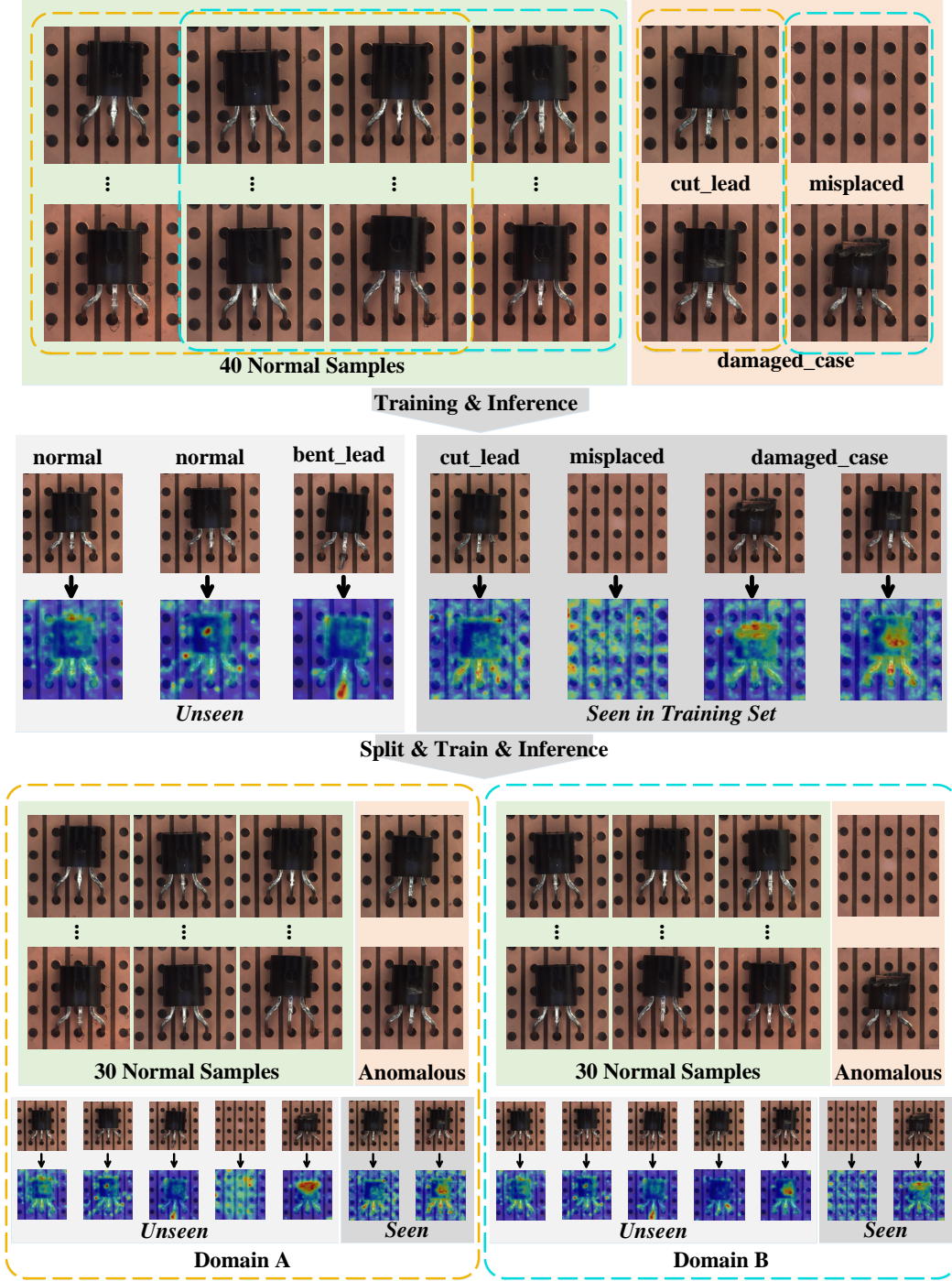


Figure A4: Results of the toy experiment for the category *transistor*.

- 24 The process consists of two steps:
- 25 (1) We create a toy train set with a noise ratio of 0.1 by sampling 40 normal samples and 4 anomalous
- 26 samples from each category, following naive RD (training the student network to learn teacher
- 27 features from all samples). We test with normal and anomalous samples not used for training and
- 28 also evaluate samples from the toy training set.

29 The results show that, compared with the anomalous samples included in the training, better anomaly  
30 maps are obtained for anomalous samples not included in the training set. This proves the applicability  
31 of RD for FUAD tasks to a certain extent. However, for some samples that have appeared during  
32 training, since the student network has learned the anomaly features of the teacher, there is a high  
33 probability that the correct anomaly maps cannot be obtained, which also corresponds to the challenge  
34 of applying RD to FUAD tasks mentioned in Sec. 3.1.

35 (2) Next, we divide the original 44 training samples into two domains. For normal samples, 50%  
36 samples are used as an overlapping portion across the two domains. For anomalous samples, we split  
37 them evenly.

38 The results indicate that, even for out-of-domain data matching in-domain anomalous patterns,  
39 such as “cut\_inner\_insulation” in cable, “color” in metal nut, and “damaged\_case” in transistor, our  
40 method generates correct anomaly maps, which validate our assumptions and support the fundamental  
41 motivation of Cross-Domain Distillation.

42 Additionally, since we use anomaly maps for visualization validation, we believe these results  
43 naturally provide a theoretical basis for extending our method to other anomaly detection paradigms.

## 44 B Results on VisA with Different Noise Ratio

45 Fig. A5 presents a comparison of the anomaly detection and localization results between our method  
46 CDD and the baseline RD as the noise ratio in the VisA dataset [8] varies from 0.3 to 0.7. Although  
47 under *No Overlap* setting, CDD does not significantly outperform RD in I-AUC and P-AUC metrics,  
48 it clearly surpasses RD in the anomaly localization metric PRO. Moreover, as the ratio of anomaly  
49 noise increases, the advantage of our method under *Overlap* setting becomes increasingly evident.

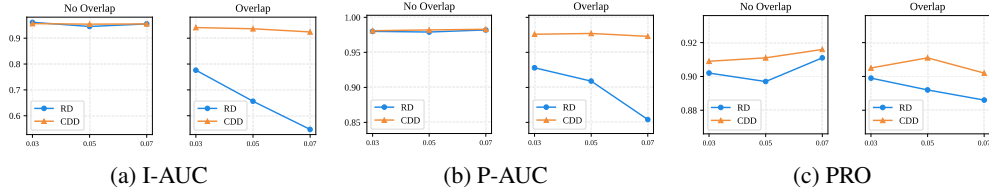


Figure A5: Comparison of anomaly detection performance with baseline RD under different  $R_{noise}$  on VisA.

## 50 C Algorithm

51 Algorithm 1 illustrates the complete training process of our proposed Cross-Domain Distillation  
52 (CDD). The input is the training set  $\mathcal{I}_{train}$ , with parameters including the total number of training  
53 epochs  $E$ , the number of domains  $K$  (dynamically adjusted during training), the maximum proportion  
54 of high-confidence samples in the training set  $r_{normal}$ , the standard deviation of Gaussian noise for  
55 feature perturbation  $\sigma_{noise}$ , and the parameter  $p$  controlling the smoothness of the regularization term  
56  $\lambda(e)$ . The output is the global student model  $S_E^{Glo}$  obtained after  $E$  epochs of training.



---

**Algorithm 1** Cross-Domain Distillation (CDD)

---

```
1: Input:  $\mathcal{I}_{train} = \{I_i\}_{i=1}^N, \mathcal{T}$ 
2: Output:  $\mathcal{S}_E^{Glo}$ 
3: Parameters:  $E, K, r_{normal} = 0.5, \sigma_{noise} = 0.2, p = 4.0$ 
4: Initialize global student  $\mathcal{S}_0^{Glo}$ 
5: for  $e = 1$  to  $E$  do
6:   Compute confidence score  $\text{Conf}_i$  for each samples  $I_i \in \mathcal{I}_{train}$  using cosine similarity
   between teacher  $\mathcal{T}$  and previous global student  $\mathcal{S}_{e-1}^{Glo}$ 
7:   Compute threshold  $r(e) = \min(\frac{e}{E}, r_{normal})$ 
8:   Sort samples by confidence, select top  $r(e) \cdot N$  as high-confidence set  $\mathcal{D}^{HC}$ 
9:   Evenly divide the rest samples into  $K$  low-confidence subsets  $\{\mathcal{D}_k^{LC}\}_{k=1}^K$ 
10:  for  $k = 1$  to  $K$  do
11:     $\mathcal{D}_k = \mathcal{D}^{HC} \cup \mathcal{D}_k^{LC}$ 
12:     $\mathcal{S}_k^{DS} \leftarrow \mathcal{S}_{e-1}^{Glo}$ 
13:    Compute the regularization weight  $\lambda(e) = \frac{(e/E)^p}{(e/E)^p + (1-e/E)^p}$ 
14:    for each  $I_i \in \mathcal{D}_k$  do
15:      Train each  $\mathcal{S}_k^{DS}$  on  $I_i$  with the loss  $\mathcal{L}_k^{DS}$  combining teacher guidance and regulariza-
      tion from  $\mathcal{S}_{e-1}^{Glo}$ , where the regularization weight is  $\lambda(e)$ 
16:    end for
17:  end for
18:  for  $k = 1$  to  $K$  do
19:    for each  $I_i \in \mathcal{D}_k$  do
20:      Extract features from other domain-specific students  $\mathcal{F}_{\mathcal{S}_h^{DS}, i}, \forall h \in \{1, \dots, K\} \setminus k$ 
      and features from previous global student  $\mathcal{F}_{\mathcal{S}_{e-1}^{Glo}, i}$ 
21:      Compute affinity to measure feature similarity  $\text{Aff}_i(h), \forall h \in \{1, \dots, K\} \setminus k$  using
       $\mathcal{F}_{\mathcal{S}_h^{DS}, i}$  and  $\mathcal{F}_{\mathcal{S}_{e-1}^{Glo}, i}$ 
22:      Select pseudo-normal feature with highest affinity  $\mathcal{F}_{pseudo, i}$ 
23:      Input teacher features with Gaussian noise  $\delta \sim \mathcal{N}(0, \sigma_{noise}^2)$  into global student  $\mathcal{S}_e^{Glo}$ 
      to get  $\mathcal{F}_{\mathcal{S}_e^{Glo}, i}^*$ 
24:      Train  $\mathcal{S}_e^{Glo}$  on sample  $I_i$  by the loss calculated using the cosine distance between
       $\mathcal{F}_{pseudo, i}$  and  $\mathcal{F}_{\mathcal{S}_e^{Glo}, i}^*$ 
25:    end for
26:  end for
27:  for each  $I_i \in \mathcal{D}^{HC}$  do
28:    Train  $\mathcal{S}_e^{Glo}$  on sample  $I_i$  by the loss calculated using teacher guidance
29:  end for
30: end for
```

---

## 57 D More Ablation Studies

### 58 D.1 Ablation Study on Parameter Selection for Confidence Threshold

59 In Sec. 4.1, we provide the formula for the confidence threshold  $r(e)$ , fixing its maximum proportion  
60 at 0.5. This choice is based on the fact that anomalous samples in real-world scenarios are typically  
61 below 50%. Setting the maximum threshold at 0.5 balances sample completeness and prevents  
62 anomaly noise from contaminating the high-confidence domain. This section validates this choice  
63 through experimental evidence, beyond just intuition.

64 Tab. A1 presents the experimental results for selecting  $r_{normal}$ . During training,  $r(e)$  is computed  
65 as  $r(e) = \min(\frac{e}{E}, r_{normal})$ . All experiments are conducted with  $K = 2$ , incorporating training  
66 strategies *D.C.*, *P.N.*, *Conf.D.* (refer to Sec. 5.3), and the domain construction strategy *Conf.G.* (refer  
67 to Sec. 5.3), which are closely tied to the confidence threshold. No other training techniques were  
68 used to avoid interference with the selection of  $r_{normal}$ .

69 We find that a smaller  $r_{normal}$  yields little improvement in performance. However, when 50% of  
70 high-confidence samples are included as normal samples in each domain, anomaly localization

improves significantly. Increasing  $r_{\text{normal}}$  further, such as to 0.7, slightly enhances anomaly detection but with minimal overall gains. Moreover, considering that there may be many abnormal scenarios in reality, and the higher the  $r_{\text{normal}}$ , the greater the consumption of training resources, we conclude that  $r_{\text{normal}} = 0.5$  offers a balanced and effective choice.

Table A1: Ablation study of  $r_{\text{normal}}$  on MVTec-noise-0.1 under *No Overlap* setting.

$r_{\text{normal}}$	I-AUC	P-AUC	PRO	Average
0.0	0.9701	0.9731	0.9225	0.9552
0.1	0.9703	0.9732	0.9187	0.9541
0.3	0.9767	0.9727	0.9187	0.9560
0.5	0.9763	0.9795	0.9224	0.9594
0.7	0.9799	0.9794	0.9201	0.9598

## D.2 Ablation Study on Regularization Hyperparameter

During domain-specific distillation to train domain-specific students, we incorporate guidance from the previous global student as a regularization term. The hyperparameter  $\lambda(e)$  for this regularization is designed as an S-shape function in Sec. 4.1. To explain this design choice, we present corresponding experimental results in Tab. A2. We compare  $\lambda(e) = 0.0$ ,  $\lambda(e) = 1.0$ , and a linear design  $\lambda(e) = e/E$ . The results show that the S-shape function achieves the best performance, while fixed or linear weights may introduce noise to the learning of domain-specific students from the global student.

Table A2: Ablation study of regularization hyperparameter  $\lambda(e)$  on MVTec-noise-0.1 under *No Overlap* setting.

$\lambda(e)$	I-AUC	P-AUC	PRO	Average
0.0	0.9802	0.9821	0.9287	0.9637
1.0	0.9768	0.9741	0.9241	0.9583
$e/E$	0.9659	0.9763	0.9225	0.9549
S-shape Function	0.9836	0.9818	0.9289	0.9648

## E Complete Quantitative Results

### E.1 Quantitative Results for Each Category on MVTec AD

Tab. A3, Tab. A4 and Tab. A5 present the image-level AUC (I-AUC), pixel-level AUC (P-AUC), and localization metric PRO for each category on the MVTec AD-noise-0.1 dataset under *No Overlap* and *Overlap* settings.

Table A3: Anomaly detection results I-AUC under *No Overlap* and *Overlap* settings on MVTec AD-noise-0.1 with the best in bold. and the second best underlined.

Setting	No Overlap							Overlap						
Method	RD [2]	ReContrast [3]	URD [6]	SoftPatch [5]	InResCh [7]	FUN-AD [4]	CDD (Ours)	RD [2]	ReContrast [3]	URD [6]	SoftPatch [5]	InResCh [7]	FUN-AD [4]	CDD (Ours)
bottle	0.997	0.994	0.992	<b>1.000</b>	<b>1.000</b>	<b>1.000</b>	<b>1.000</b>	0.742	0.687	0.680	<b>1.000</b>	0.999	<b>1.000</b>	<b>1.000</b>
cable	0.931	0.977	0.955	<b>0.996</b>	0.958	0.952	<u>0.981</u>	0.709	0.743	0.727	<b>0.995</b>	0.871	0.963	<u>0.970</u>
capsule	0.939	<u>0.959</u>	0.951	<b>0.961</b>	0.446	0.922	0.942	0.788	0.835	0.785	0.957	0.456	<u>0.925</u>	<b>0.939</b>
carpet	0.985	<b>1.000</b>	0.993	0.989	0.980	<b>1.000</b>	0.989	0.675	<b>1.000</b>	0.681	0.992	0.978	<b>1.000</b>	0.990
grid	0.956	<b>1.000</b>	<b>1.000</b>	0.965	0.917	0.991	<b>1.000</b>	0.947	0.998	0.817	0.971	0.928	<u>0.995</u>	<b>1.000</b>
hazelnut	<b>1.000</b>	0.999	0.994	<b>1.000</b>	0.997	0.999	<b>1.000</b>	0.443	0.450	0.454	<b>1.000</b>	0.951	<b>1.000</b>	0.986
leather	<b>1.000</b>	<b>1.000</b>	<b>1.000</b>	<b>1.000</b>	<b>1.000</b>	<b>1.000</b>	<b>1.000</b>	0.762	0.876	0.750	<b>1.000</b>	0.993	<b>1.000</b>	<b>1.000</b>
metal_nut	0.988	0.999	0.994	0.998	0.970	0.997	<b>1.000</b>	0.755	0.763	0.759	<b>0.999</b>	0.935	0.998	0.968
pill	0.960	<b>0.991</b>	0.961	0.953	0.889	0.939	0.971	0.783	0.857	0.784	<u>0.959</u>	0.812	0.946	<b>0.963</b>
screw	<b>0.980</b>	<u>0.979</u>	0.954	0.952	0.779	0.913	0.934	0.716	0.768	0.698	<b>0.934</b>	0.678	0.910	0.849
tile	0.988	0.992	<b>1.000</b>	<b>1.000</b>	0.999	0.999	0.997	0.717	0.720	0.726	<u>0.990</u>	0.982	<b>0.996</b>	0.970
toothbrush	<b>1.000</b>	<b>1.000</b>	<b>1.000</b>	<b>1.000</b>	0.990	0.972	0.997	0.803	0.800	0.800	<b>1.000</b>	0.964	0.961	<u>0.997</u>
transistor	0.943	0.950	0.948	<u>0.996</u>	0.929	0.962	<b>0.998</b>	0.448	0.451	0.450	<b>0.996</b>	0.823	0.968	<b>0.996</b>
wood	0.990	0.990	0.994	<u>0.997</u>	0.947	<b>1.000</b>	0.993	0.594	0.615	0.630	<u>0.990</u>	0.868	<b>1.000</b>	0.985
zipper	0.924	<u>0.983</u>	0.861	0.974	0.952	<b>0.984</b>	0.958	0.745	0.856	0.699	<u>0.973</u>	0.946	<b>0.983</b>	0.957
Average	0.972	<b>0.988</b>	0.973	<u>0.985</u>	0.917	0.975	0.984	0.708	0.761	0.696	<b>0.984</b>	0.879	<u>0.976</u>	0.971

Table A4: Anomaly localization results P-AUC under *No Overlap* and *Overlap* settings on MVTec AD-noise-0.1 with the best in bold. and the second best underlined.

Setting	No Overlap							Overlap						
Method	RD [2]	ReContrast [3]	URD [6]	SoftPatch [5]	InReaCh [7]	FUN-AD [4]	CDD (Ours)	RD [2]	ReContrast [3]	URD [6]	SoftPatch [5]	InReaCh [7]	FUN-AD [4]	CDD (Ours)
bottle	0.983	0.984	0.984	0.988	0.981	<b>0.992</b>	0.987	0.917	0.902	0.854	<u>0.983</u>	0.972	<b>0.991</b>	0.982
cable	0.835	0.924	0.881	<b>0.989</b>	<u>0.978</u>	0.920	0.969	0.727	0.828	0.753	<b>0.981</b>	0.957	0.931	<u>0.962</u>
capsule	0.980	0.976	0.981	<b>0.990</b>	0.914	<u>0.987</u>	0.984	0.889	0.917	0.878	<b>0.989</b>	0.861	<u>0.986</u>	0.978
carpet	0.988	0.990	0.991	0.991	<u>0.992</u>	<b>0.995</b>	0.989	0.732	<u>0.990</u>	0.717	<u>0.990</u>	0.987	<b>0.994</b>	0.988
grid	<b>0.994</b>	0.990	0.990	0.992	0.983	<u>0.993</u>	0.992	<b>0.990</b>	0.984	0.952	0.972	0.975	<b>0.990</b>	0.989
hazelnut	0.992	0.992	<b>0.993</b>	<b>0.993</b>	0.988	0.991	<b>0.993</b>	0.774	0.870	0.768	0.887	0.965	<b>0.992</b>	<u>0.983</u>
leather	0.995	0.996	0.995	0.994	0.992	<b>0.998</b>	0.991	0.848	0.941	0.775	0.993	0.990	<b>0.998</b>	0.990
metal_nut	0.833	0.870	0.848	0.857	0.958	<b>0.992</b>	<u>0.962</u>	0.736	0.796	0.719	<u>0.856</u>	0.925	<b>0.993</b>	<u>0.960</u>
pill	0.966	<b>0.985</b>	0.956	<u>0.981</u>	0.956	0.972	0.978	0.889	0.971	0.838	<u>0.975</u>	0.942	0.971	<b>0.976</b>
screw	<b>0.995</b>	<u>0.994</u>	<u>0.994</u>	0.982	0.981	0.992	0.985	<u>0.974</u>	0.803	0.961	0.964	0.964	<b>0.981</b>	<u>0.974</u>
tile	0.961	<u>0.969</u>	0.964	0.965	0.965	<b>0.978</b>	0.955	0.823	0.834	0.820	<u>0.957</u>	0.955	<b>0.980</b>	0.946
toothbrush	0.991	<b>0.992</b>	<b>0.992</b>	0.987	0.989	0.981	0.987	0.953	0.929	0.952	<b>0.985</b>	<b>0.985</b>	0.979	0.984
transistor	0.882	0.917	0.901	0.972	<b>0.982</b>	0.975	<u>0.980</u>	0.587	0.720	0.526	0.922	0.911	<u>0.953</u>	<b>0.961</b>
wood	0.978	<u>0.982</u>	<b>0.983</b>	0.938	0.962	0.977	0.979	0.658	0.723	0.671	0.917	0.874	<b>0.957</b>	<u>0.945</u>
zipper	0.976	0.977	0.973	<b>0.988</b>	0.937	0.970	0.980	0.888	0.922	0.853	<b>0.986</b>	0.881	0.962	<u>0.971</u>
Average	0.957	0.969	0.962	0.975	0.971	<u>0.980</u>	<b>0.981</b>	0.818	0.887	0.792	0.957	0.943	<b>0.977</b>	<u>0.973</u>

Table A5: Anomaly localization results PRO under *No Overlap* and *Overlap* settings on MVTec AD-noise-0.1 with the best in bold. and the second best underlined.

Setting	No Overlap							Overlap						
Method	RD [2]	ReContrast [3]	URD [6]	SoftPatch [5]	InReaCh [7]	FUN-AD [4]	CDD (Ours)	RD [2]	ReContrast [3]	URD [6]	SoftPatch [5]	InReaCh [7]	FUN-AD [4]	CDD (Ours)
bottle	0.955	0.958	<b>0.961</b>	0.956	0.915	<u>0.960</u>	0.959	0.928	0.947	0.947	<u>0.954</u>	0.917	<b>0.963</b>	0.949
cable	0.768	0.847	0.824	<b>0.919</b>	0.862	0.740	<u>0.891</u>	0.740	0.825	0.812	<b>0.918</b>	0.850	0.770	<u>0.888</u>
capsule	0.956	0.953	<u>0.958</u>	<b>0.965</b>	0.657	0.855	0.950	0.953	0.947	<u>0.956</u>	<b>0.959</b>	0.599	0.862	0.940
carpet	0.957	<u>0.968</u>	<b>0.972</b>	0.959	0.958	0.953	0.960	0.932	<b>0.973</b>	0.915	0.966	0.962	0.954	<u>0.967</u>
grid	<b>0.979</b>	<u>0.978</u>	0.976	0.963	0.929	0.935	0.976	0.966	<b>0.975</b>	0.965	0.949	0.914	0.932	<u>0.971</u>
hazelnut	0.936	0.931	<b>0.953</b>	0.942	0.907	0.885	<u>0.945</u>	0.930	<u>0.937</u>	<b>0.948</b>	0.879	0.898	0.883	0.936
leather	0.988	<b>0.991</b>	0.990	0.988	0.985	0.986	0.971	0.988	<b>0.991</b>	0.985	0.988	0.981	0.985	0.970
metal_nut	0.859	0.870	0.869	0.838	<b>0.887</b>	0.864	0.870	0.830	0.877	0.865	0.832	0.869	<b>0.879</b>	0.858
pill	0.956	<b>0.969</b>	0.950	0.945	0.883	0.893	<u>0.958</u>	0.957	<b>0.969</b>	<u>0.951</u>	0.942	0.886	0.892	0.947
screw	<b>0.983</b>	0.977	<u>0.977</u>	0.975	0.936	0.772	0.974	<b>0.978</b>	<u>0.976</u>	0.975	0.923	0.923	0.788	<u>0.976</u>
tile	0.858	0.894	<u>0.897</u>	0.878	0.878	<b>0.939</b>	0.879	0.861	0.883	0.822	0.874	0.863	<b>0.939</b>	<u>0.887</u>
toothbrush	0.939	<u>0.940</u>	<b>0.943</b>	0.915	0.904	0.850	0.916	0.918	<u>0.937</u>	<b>0.938</b>	0.892	0.899	0.829	0.907
transistor	0.753	0.786	0.812	0.819	0.786	0.520	<b>0.831</b>	0.700	0.718	0.738	<u>0.786</u>	0.758	0.505	<b>0.788</b>
wood	0.906	<u>0.924</u>	<u>0.924</u>	0.912	0.875	<b>0.960</b>	0.916	0.888	<u>0.920</u>	0.889	0.890	0.840	<b>0.957</b>	0.889
zipper	0.941	0.938	0.926	<b>0.969</b>	0.796	0.925	<u>0.950</u>	<u>0.942</u>	0.924	0.922	<b>0.967</b>	0.752	0.916	0.938
Average	0.916	0.928	0.929	<b>0.930</b>	0.877	0.869	<b>0.930</b>	0.901	<u>0.920</u>	0.909	0.915	0.861	0.870	<b>0.921</b>

## 87 E.2 Quantitative Results for Each Category on VisA

88 Tab. A6, Tab. A7 and Tab. A8 present the image-level AUC (I-AUC), pixel-level AUC (P-AUC), and  
89 localization metric PRO for each category on the VisA-noise-0.05 dataset under *No Overlap* and  
90 *Overlap* settings.

Table A6: Anomaly detection results I-AUC under *No Overlap* and *Overlap* settings on VisA-noise-0.05 with the best in bold. and the second best underlined.

Setting	No Overlap					Overlap				
Method	RD [2]	SoftPatch [5]	InReaCh [7]	FUN-AD [4]	CDD (Ours)	RD [2]	SoftPatch [5]	InReaCh [7]	FUN-AD [4]	CDD (Ours)
candle	0.928	<b>0.978</b>	0.936	0.931	<u>0.954</u>	0.617	<b>0.977</b>	0.770	0.938	<u>0.948</u>
capsules	0.800	0.716	0.548	<b>0.886</b>	<u>0.807</u>	0.577	0.695	0.496	<b>0.885</b>	<u>0.735</u>
cashew	0.962	<u>0.975</u>	0.850	0.945	<b>0.984</b>	0.751	<u>0.970</u>	0.809	0.943	<b>0.983</b>
chewinggum	0.978	<b>0.987</b>	0.747	<u>0.980</u>	0.977	0.763	<b>0.988</b>	0.716	<u>0.983</u>	0.982
fryum	<b>0.979</b>	0.944	0.873	0.953	0.966	0.794	0.944	0.837	<u>0.951</u>	<b>0.965</b>
macaroni1	0.977	0.960	0.861	0.936	<b>0.983</b>	0.696	<b>0.956</b>	0.656	<u>0.950</u>	0.937
macaroni2	0.810	0.675	0.660	0.775	<b>0.873</b>	0.565	0.680	0.488	<u>0.802</u>	<b>0.825</b>
pcb1	0.979	<u>0.980</u>	0.645	0.934	<b>0.984</b>	0.539	<u>0.971</u>	0.600	0.942	<b>0.978</b>
pcb2	<b>0.945</b>	0.934	0.921	0.896	<u>0.944</u>	0.561	<u>0.944</u>	0.889	0.927	<b>0.952</b>
pcb3	<b>0.988</b>	0.982	0.946	0.888	<u>0.983</u>	0.590	<b>0.971</b>	0.706	0.912	<u>0.946</u>
pcb4	0.996	<b>0.997</b>	0.980	0.968	<b>0.997</b>	0.647	<u>0.997</u>	0.924	0.974	<b>0.998</b>
pipe_fryum	<b>0.995</b>	0.992	0.962	<u>0.994</u>	0.992	0.776	<u>0.993</u>	0.809	<b>0.995</b>	0.984
Average	<u>0.945</u>	0.927	0.827	0.924	<b>0.954</b>	0.656	0.924	0.725	<u>0.934</u>	<b>0.936</b>



Table A7: Anomaly localization results P-AUC under *No Overlap* and *Overlap* settings on VisA-noise-0.05 with the best in bold. and the second best underlined.

Setting	No Overlap					Overlap				
Method	RD [2]	SoftPatch [5]	InReaCh [7]	FUN-AD [4]	CDD (Ours)	RD [2]	SoftPatch [5]	InReaCh [7]	FUN-AD [4]	CDD (Ours)
candle	0.989	<b>0.995</b>	0.987	0.990	0.992	0.956	<b>0.993</b>	0.851	0.989	0.986
capsules	<b>0.990</b>	0.985	0.949	<b>0.990</b>	0.987	0.826	0.961	0.887	<b>0.989</b>	<u>0.987</u>
cashew	0.937	<u>0.986</u>	0.983	<b>0.993</b>	0.938	0.931	<u>0.986</u>	0.974	<b>0.993</b>	0.937
chewinggum	0.970	<u>0.989</u>	0.920	<b>0.993</b>	0.982	0.837	<u>0.990</u>	0.914	<b>0.993</b>	0.978
fryum	0.941	0.924	<b>0.959</b>	<u>0.951</u>	0.942	0.908	0.918	<u>0.949</u>	<b>0.951</b>	0.942
macaroni1	0.994	<b>0.998</b>	0.979	0.994	<b>0.998</b>	0.980	<b>0.996</b>	0.857	0.994	<u>0.995</u>
macaroni2	0.986	<u>0.987</u>	0.968	0.982	<b>0.995</b>	0.936	0.743	0.831	<u>0.984</u>	<b>0.986</b>
pcb1	0.994	<b>0.999</b>	0.996	0.995	0.992	0.885	<b>0.998</b>	0.946	<u>0.993</u>	0.986
pcb2	0.983	<b>0.985</b>	0.977	0.953	<b>0.985</b>	0.912	<u>0.968</u>	0.916	0.959	<b>0.978</b>
pcb3	0.995	<b>0.996</b>	0.990	0.982	0.995	0.960	<b>0.992</b>	0.954	0.966	0.990
pcb4	<b>0.987</b>	<b>0.987</b>	0.985	0.986	0.986	0.871	0.917	0.904	<b>0.981</b>	0.979
pipe_fryum	0.985	0.989	<b>0.994</b>	<u>0.993</u>	0.987	0.905	<u>0.989</u>	0.982	<b>0.993</b>	0.984
Average	0.979	<b>0.985</b>	0.974	<u>0.984</u>	0.982	0.909	0.954	0.914	<b>0.982</b>	<u>0.977</u>

Table A8: Anomaly localization results PRO under *No Overlap* and *Overlap* settings on VisA-noise-0.05 with the best in bold. and the second best underlined.

Setting	No Overlap					Overlap				
Method	RD [2]	SoftPatch [5]	InReaCh [7]	FUN-AD [4]	CDD (Ours)	RD [2]	SoftPatch [5]	InReaCh [7]	FUN-AD [4]	CDD (Ours)
candle	0.911	<b>0.928</b>	0.918	0.801	<b>0.928</b>	0.911	<b>0.946</b>	0.861	0.831	<u>0.939</u>
capsules	<u>0.941</u>	0.831	0.655	0.836	<b>0.950</b>	<u>0.944</u>	0.735	0.607	0.819	<b>0.958</b>
cashew	0.810	<b>0.940</b>	0.521	<u>0.891</u>	0.867	0.790	<b>0.937</b>	0.462	<u>0.875</u>	0.866
chewinggum	0.749	<b>0.883</b>	0.451	<u>0.820</u>	0.819	0.731	<b>0.884</b>	0.426	0.809	<u>0.812</u>
fryum	<b>0.893</b>	0.825	0.797	0.699	<u>0.886</u>	<b>0.899</b>	0.816	0.785	0.695	<u>0.889</u>
macaroni1	0.954	<u>0.968</u>	0.876	0.892	<b>0.972</b>	0.938	<u>0.965</u>	0.798	0.863	<b>0.974</b>
macaroni2	0.903	0.902	0.860	0.800	<b>0.967</b>	0.916	0.800	0.722	0.801	<b>0.971</b>
pcb1	<b>0.945</b>	<u>0.944</u>	0.899	0.778	0.913	<u>0.901</u>	<b>0.919</b>	0.671	0.721	0.887
pcb2	<b>0.881</b>	<u>0.874</u>	0.844	0.658	0.872	<b>0.890</b>	0.873	0.761	0.682	<u>0.875</u>
pcb3	<b>0.946</b>	0.931	0.903	0.842	0.934	<b>0.940</b>	0.923	0.862	0.828	<u>0.936</u>
pcb4	<b>0.879</b>	0.861	0.832	0.646	<u>0.864</u>	<b>0.896</b>	0.846	0.758	0.707	<u>0.875</u>
pipe_fryum	0.956	<u>0.961</u>	<b>0.962</b>	0.895	0.955	<b>0.952</b>	<b>0.952</b>	0.940	0.883	0.947
Average	0.897	<u>0.904</u>	0.793	0.797	<b>0.911</b>	<u>0.892</u>	0.883	0.721	0.793	<b>0.911</b>

## F More Qualitative Results

### F.1 Qualitative Results on MVTec

Figure A6 provides a visualization comparison of anomaly maps generated by FUAD methods, including SoftPatch [5], InReaCh [7], the baseline RD [2], and our proposed CDD, all trained on MVTec AD-noise-0.1. The samples, drawn from the test set under *No Overlap* setting, highlight that our method, especially compared to the baseline RD, effectively localizes anomalies.

### F.2 Qualitative Results on VisA

Similar to Fig. 4, we calculate anomaly scores for samples in the training and test set of VisA-noise-0.05, resulting in the anomaly score distribution histograms shown in Fig. A7. These histograms demonstrate that, compared to the baseline RD [2], our proposed method generates anomaly scores that more effectively distinguish between anomalous and normal samples.

Additionally, we compared the anomaly maps of our CDD with SoftPatch [5], InReaCh [7], and the baseline RD [2] on VisA-noise-0.05 in Fig. A8, showing that our method consistently achieves effective anomaly localization across various scenarios.

### F.3 Qualitative Results on Hard Samples

In FUAD tasks, it is challenging for a trained model to localize anomalies for the anomalous samples in the training set, which led to the introduction of the *Overlap* setting. Therefore, we conduct visualizations by generating anomaly maps for the anomalous samples selected from the training set. Figure A9 and Figure A10 compare anomaly maps from SoftPatch [5], the baseline RD [2], and our CDD on MVTec AD-noise-0.1 and VisA-noise-0.05, respectively. The results show that our method, through cross-domain training, effectively mitigates the noise interference from training set and achieves accurate anomaly localization even on training samples.

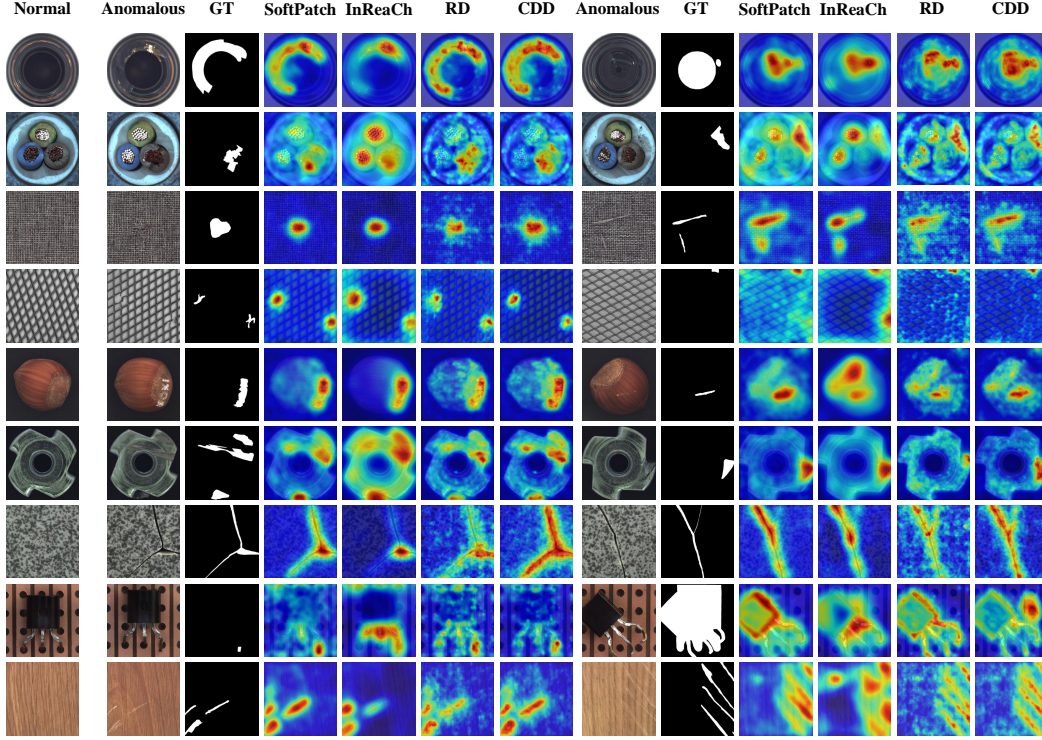


Figure A6: Visualization comparison of anomaly maps generated by FUAD methods SoftPatch [5], InReaCh [7], the baseline RD [2], and our proposed CDD trained on MVTec AD-noise-0.1. All the samples are obtained from the test set under *No Overlap* setting.

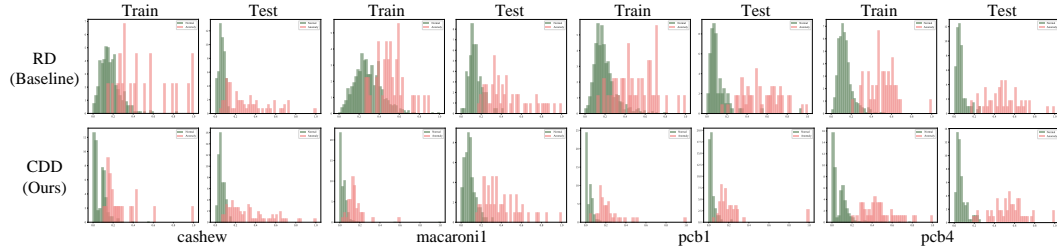


Figure A7: Comparison of histograms of anomaly scores obtained by RD and our CDD. on VisA-noise-0.05.

## 113 G More Discussions

114 In Sec. 6, we discuss the current limitations of CDD, noting that it has not been extended to more  
 115 paradigms and remains confined within the RD framework.

116 In addition, our method currently employs random domain division, which introduces strong random-  
 117 ness and may result in clustering the same anomaly type into a single domain, potentially violating  
 118 *Assumption 1*. Although *Assumption 2* still allows us to achieve results surpassing the baseline, this  
 119 randomness somewhat limits the method’s effectiveness.

120 In future work, we plan to extend this Cross-Domain idea for FUAD to other anomaly detection  
 121 paradigms, such as feature reconstruction, and apply pre-processing techniques like data clustering  
 122 before domain construction to ensure the reliability of the process.

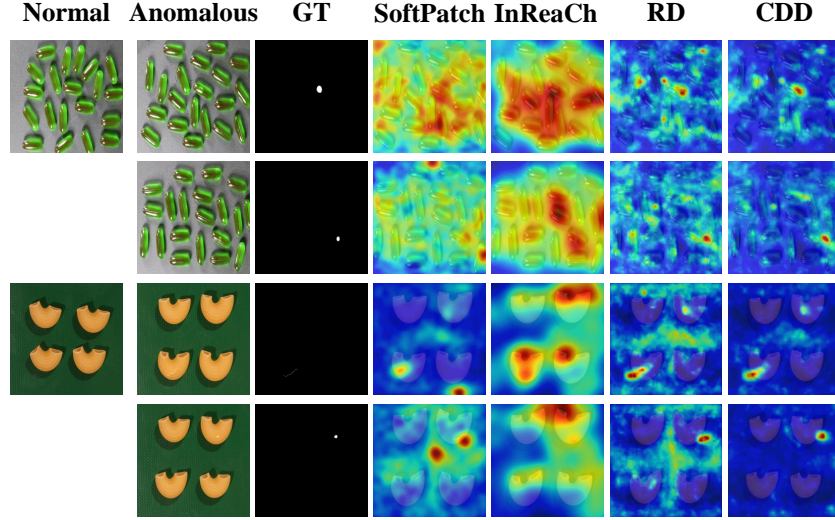


Figure A8: Visualization comparison of anomaly maps generated by FUAD methods SoftPatch [5], InReaCh [7], the baseline RD [2], and our proposed CDD trained on VisA-noise-0.05. All the samples are obtained from the test set under *No Overlap* setting.

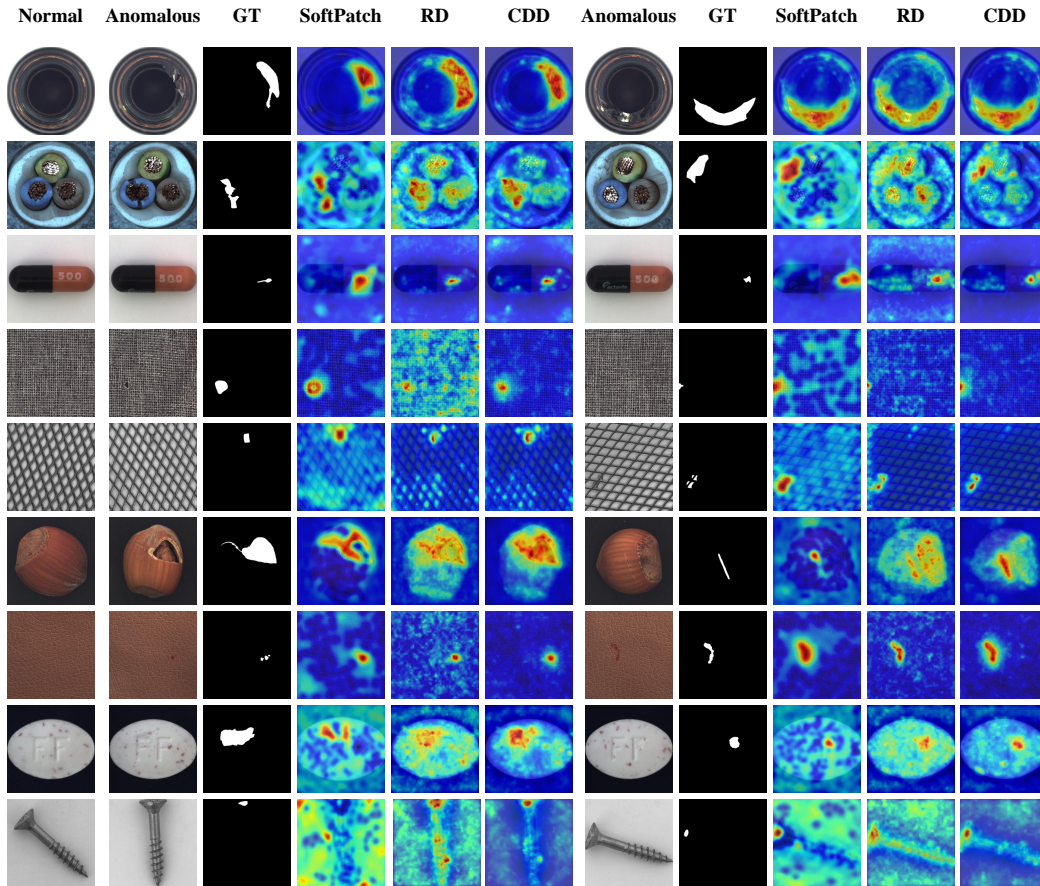


Figure A9: Visualization comparison of anomaly maps generated by FUAD methods SoftPatch [5], the baseline RD [2], and our proposed CDD trained on MVTec AD-noise-0.1. All the anomalous samples are obtained from the train set.



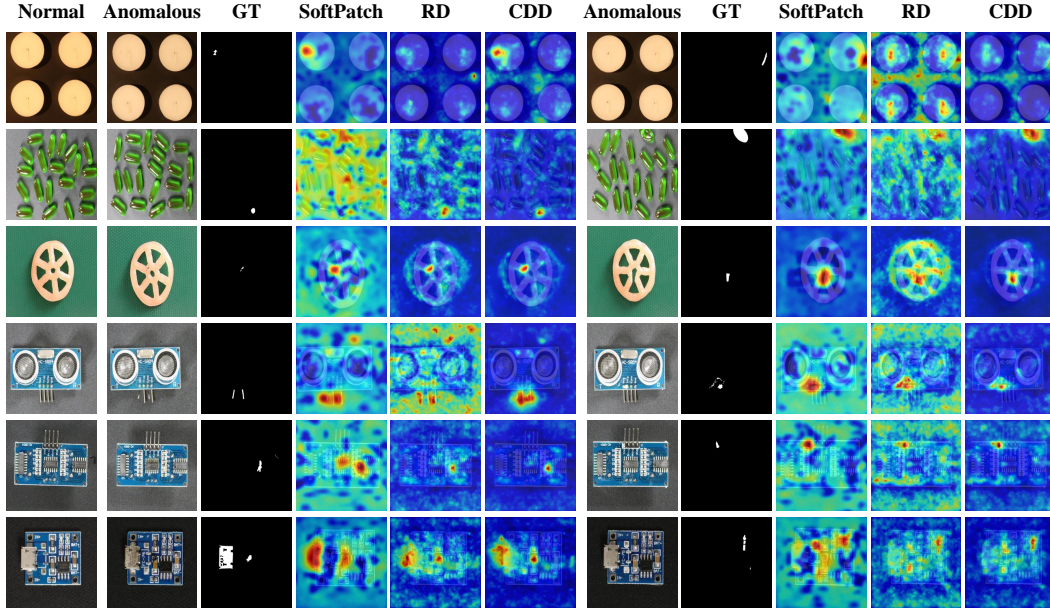


Figure A10: Visualization comparison of anomaly maps generated by FUAD methods SoftPatch [5], the baseline RD [2], and our proposed CDD trained on VisA-noise-0.05. All the anomalous samples are obtained from the train set.

## References

- [1] P. Bergmann, M. Fauser, D. Sattlegger, and C. Steger. Mvtec ad—a comprehensive real-world dataset for unsupervised anomaly detection. In *Proceedings of the IEEE/CVF conference on computer vision and pattern recognition*, pages 9592–9600, 2019.
- [2] H. Deng and X. Li. Anomaly detection via reverse distillation from one-class embedding. In *Proceedings of the IEEE/CVF Conference on Computer Vision and Pattern Recognition*, pages 9737–9746, 2022.
- [3] J. Guo, L. Jia, W. Zhang, H. Li, et al. Recontrast: Domain-specific anomaly detection via contrastive reconstruction. *Advances in Neural Information Processing Systems*, 36, 2024.
- [4] J. Im, Y. Son, and J. H. Hong. Fun-ad: Fully unsupervised learning for anomaly detection with noisy training data. In *2025 IEEE/CVF Winter Conference on Applications of Computer Vision (WACV)*, pages 9447–9456. IEEE, 2025.
- [5] X. Jiang, J. Liu, J. Wang, Q. Nie, K. Wu, Y. Liu, C. Wang, and F. Zheng. Softpatch: Unsupervised anomaly detection with noisy data. *Advances in Neural Information Processing Systems*, 35:15433–15445, 2022.
- [6] X. Liu, J. Wang, B. Leng, and S. Zhang. Unlocking the potential of reverse distillation for anomaly detection. In *Proceedings of the AAAI Conference on Artificial Intelligence*, volume 39, pages 5640–5648, 2025.
- [7] D. McIntosh and A. B. Albu. Inter-realization channels: Unsupervised anomaly detection beyond one-class classification. In *Proceedings of the IEEE/CVF International Conference on Computer Vision*, pages 6285–6295, 2023.
- [8] Y. Zou, J. Jeong, L. Pemula, D. Zhang, and O. Dabeer. Spot-the-difference self-supervised pre-training for anomaly detection and segmentation. In *European Conference on Computer Vision*, pages 392–408. Springer, 2022.